Mineralogical and Geochemical Study of the Asmari Group in the Fauqi Oil Field in Maysan, Southeastern Iraq

Muataz J. Al-Mishkil[1, *], Harith A. Al-Saad[1] and Fahad M. Al-Najm [1]

[1]   Department of Geology, College of Science, University of Basrah, Iraq
*   **Correspondence**: mautzgeo@gmail.com

Abstract

The presence of clay minerals of any kind and in any quantity and distribution pattern in hydrocarbon wells causes many problems in the qualitative assessment of the reservoir, A geochemical and mineralogical study are conducted on the reservoir units of the Asmari Group (early Miocene-Oligocene) to identify the clay mineral types present in the reservoir and the effect these clay minerals have on the reservoir's petrophysical properties. the Jeribe Formation (unit A) and the Upper Kirkuk Formation (unit B) are represented the main units of the Asmari reservoir ten samples from the Asmari group of the Fauqi oil field were chosen: five from the southern dome denoted by a number 65 and the same from the northern dome denoted by a number 64, Samples 1 and 2 represent unit A, while samples 3, 4, and 5 represent unit B. The mineralogical study showed that the non-clay minerals are represented by dolomite, calcite, anhydrite, quartz, and halite, while the clay minerals are represented by Illite, kaolinite, and chlorite, the geochemical analysis showed that the main oxides in the reservoir units of the Al-Asmari group are: silica, alumina, iron oxide, calcium oxide, magnesium oxide, sodium oxide, potassium oxide, titanium dioxide, sulfate, and chlorine, the highest percentage of the main oxides are calcium oxide, sulfate, and silica, respectively, and that the northern dome has a higher percentage of calcium, magnesium, sulfate, and the loss of ignition than the southern dome, while the percentage of silica and alumina in the southern dome is higher than its percentage in the northern dome which indicates a high percentage of clay minerals in the southern dome. The positive correlation between potassium and sodium and the negative correlation between potassium and calcium indicates that the Illite is of the Na-Illite type. Due to its lower charge Na and weak hydrogen bonds, Na-illite has greater dispersibility than Ca-illite and is present in all samples, making it the most clay mineral affecting the petrophysical properties in the study area.

Keywords: Geochemical data; Mineralogy; Clay minerals; Asmari group; Fauqi oil field

1. Introduction

Tertiary age is extremely significant in Iraq and Iran due to the presence of numerous geological formations with economic significance and the presence of rocks with good hydrocarbon reservoir characteristics.

The Oligocene-Miocene Asmari group is one of the most important oil reserve groups in the Zagros Basin, which is south and southwest of Iran and southeast and north of Iraq and is found in the Fauqi and Abu Ghirab oil fields (Luo et al., 2019), specifically in the Unstable Shelf, foothill zone, in the Hemrin-Makhul zone according to the longitudinal division of Iraq, and the Mesopotamian block According to the transversal division of Iraq, it is bounded from the north by the Sirwan Fault, and from the south by the Takhadid-Qurna Fault (Jassim and Goff, 2006). Structurally, the Fauqi field represents the anticline fold non-cylindrical, which contains many culminations. The north and south parts of the field are separated by depressions along the NW-SE fold axis. The whole form of the structure tends to be the so-called gradual fold (Enechelon fold).

The study is focused on the Asmari group in the Fauqi oil field, which is in the Mission Province in southeast Iraq, near the Iraqi Iranian border, approximately 50 kilometers northeast of the city of Amara, 350 kilometres southeast of Baghdad, and 175 kilometers north of Basrah (Fig1). The Asmari group in the Fauqi oil field is divided into four formations, which are: (unit A) Jeribe-Euphrates; (unit B) Upper Kirkuk; (unit C) Buzurgan Member; and (unit D) Middle-Lower Kirkuk (Al-Baldawi, 2015).

Ten samples from units A and B have been selected for two purposes: mineral analysis, to know the different types of minerals (nonclay minerals and clay minerals), and geochemical analysis, to determine the percentage of major oxides in these units because they are important units as the oil-bearing reservoir units. The presence of clay minerals in a reservoir affects reservoir characteristics such as porosity and permeability. each type of clay mineral has a different effect on reservoir properties, such as the swell effect of montmorillonite, the dispersal and migration of kaolinite and illite in addition to montmorillonite, and the transformation of clay minerals into other mineral phases (Merriman, 2005), and due to the fact that clay minerals are impacted by physical and chemical changes in the environment throughout the deposition process and transform into different minerals as a result of these changes (Al-Amery and Al-Saad, 2022). Therefore, clay minerals have been studied to comprehend the effects of their presence in the Asmari reservoir.

2. Materials and Methods

2.1. Mineralogy

Based on the anomalies in the spectral gamma-ray log behavior, ten samples from the Asmari group of the Fauqi oil field were chosen: five from the southern dome and the same number from the northern dome. Samples 1 and 2 represent unit A, while samples 3, 4, and 5 represent unit B, and the samples from the northern dome have the number 64, and samples from the southern dome have the number 65. The main objective of the mineralogy study was to identify and characterize the major clay minerals present in the Asmari reservoir. This was done using an X-ray diffraction device of a type (MPD from Panalytical Business, X-Pert Pro) at the Faculty of Science, University of Basrah.

Non-clay mineral content is determined by powdering 10 bulk samples, as recommended by (Folk, 1968), (Carroll, 1970), (Gibbs, 1968), and (Gibbs, 1968). In addition, from the same previous samples, oriented slides are created after the clay minerals are separated from the samples and studied for normal, heated, and ethylene glycol analysis to determine the types of clay minerals, that have been subjected to Scans in the $2\theta°$ angular range between (2°-40°) for non-clay minerals and (2°-20°) for clay minerals. Also has used spectral gamma ray logs to identify clay minerals through the cross-plots and ratio of thorium and potassium spectral gamma ray logs, which measure the natural radioactivity of Formations (concentrations of potassium, thorium, and uranium in formation rocks). so, each type of clay mineral

can be determined depending on the ratio of TH/K by the intersection of potassium and thorium using special charts prepared by Schlumberger Company (Schlumberger, 2009) Where the gradients of the lines emerging from the plot correspond to the Th/K ratio values which calculated for each clay mineral (Klaja and Dudek, 2016) (Table 1.)
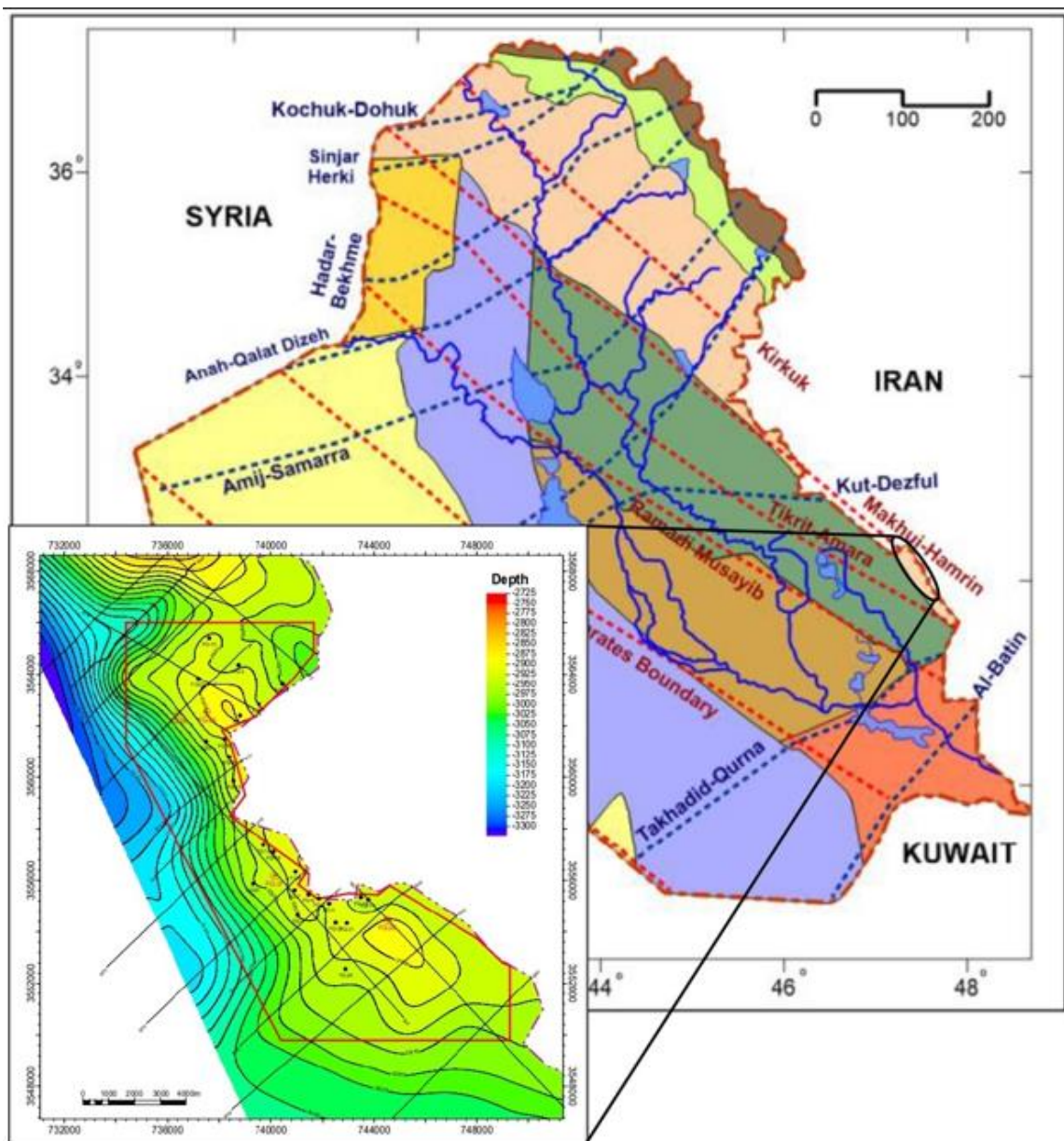
Fig.1. The location map of the study area in the Fauqi oilfield

Table 1. Classification of clay minerals based on Th/K (Klaja and Dudek, 2016)

No.	Th (ppm)/K (%)	Minerals
1	< 0.6	Feldspars
2	0.6–1.5	Glauconite
3	1.5–2.0	Micas
4	2.0–3.5	Illite
5	> 3.5	Mixed-layer clays
6	Ten and above	Kaolinite and chlorite

2.2. Geochemistry

The percentage of major oxides in ten Asmari Formation samples was determined through geochemical analysis using XRD-Fluorescence type (spectry xepos X-ray) at the Iraqi-German laboratory of the Geological Department of the College of Science, University of Baghdad, before performing the geochemical analysis. The samples are first ground to a powder with a particle size of less than 75 microns (200 mesh), and the powder is then formed into tablets using a five-ton press so that they are ready for analysis.

3. Results and Discussion

3.1. Mineralogy

The mineral composition of Asmari reservoir samples has been determined using X-ray diffraction analyses, which show that the non-clay minerals are dolomite at the base reflection (2.8 Å), calcite at the base reflection (3.03 Å), quartz at the base reflection (4.2 Å, 3.3 Å, 2.2 Å) respectively, anhydrite at the base reflection (3.4 Å), and halite at a base reflection, (2.7 Å) (Fig. 2) and for clay minerals (Fig. 3)
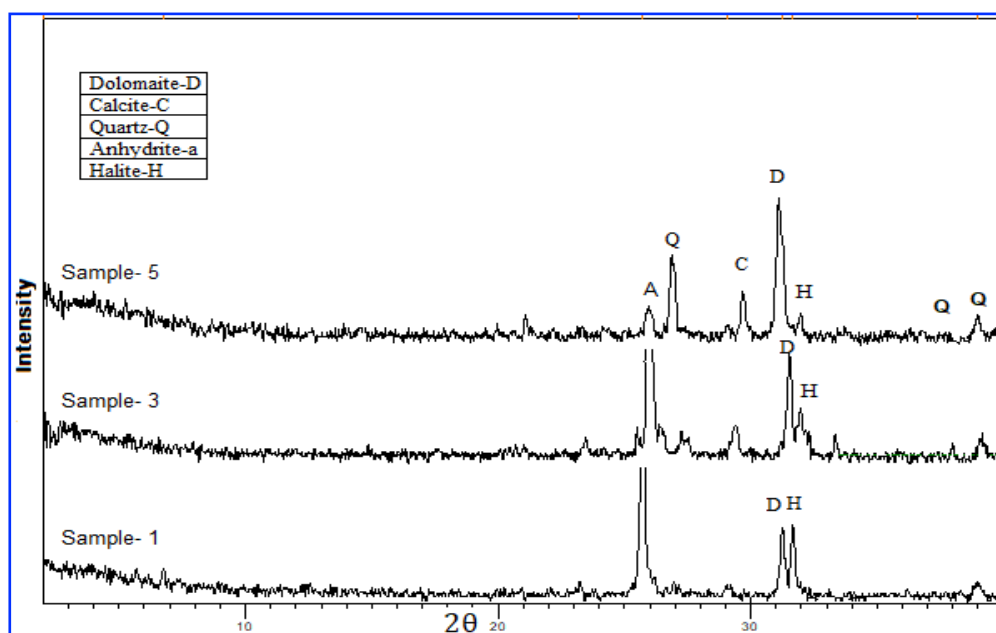
Fig. 2. X-ray diffraction reveals non-clay minerals in the study area.
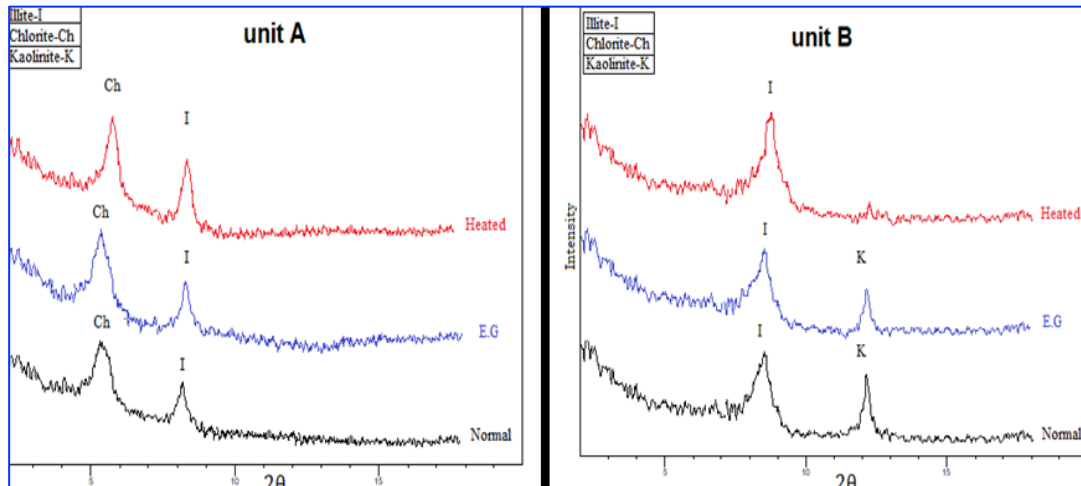
Fig. 3. X-ray diffraction shows the presence of clay minerals in the study area.

The Illite is detected by using X-ray diffraction at the basal reflection (10.5) (Fig. 3), and by cross-plot between thorium and potassium, the Illite has an average TH/K ratio in unit A is 2.6 for the southern dome, and 2.8 for the northern dome, while the average TH/K ratio in unit B is 3.2 for the southern dome, the average TH/K ratio is 3.2 for the northern dome (Figs. 4 and 5) and (Table 2).
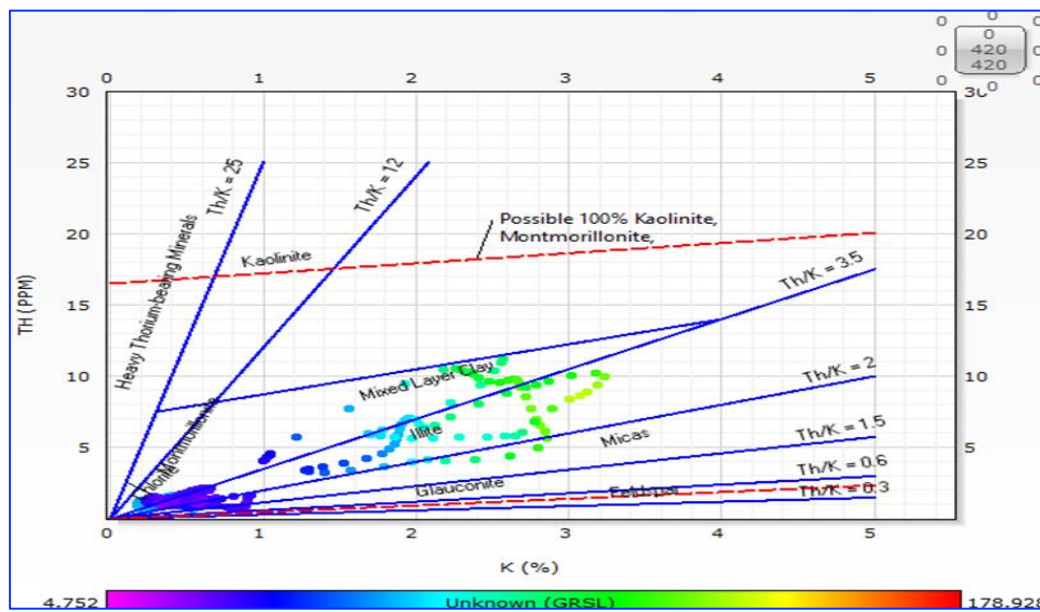
Fig. 4. Cross plot of thorium - potassium, used to identify clay minerals of selected samples from the unit (A)
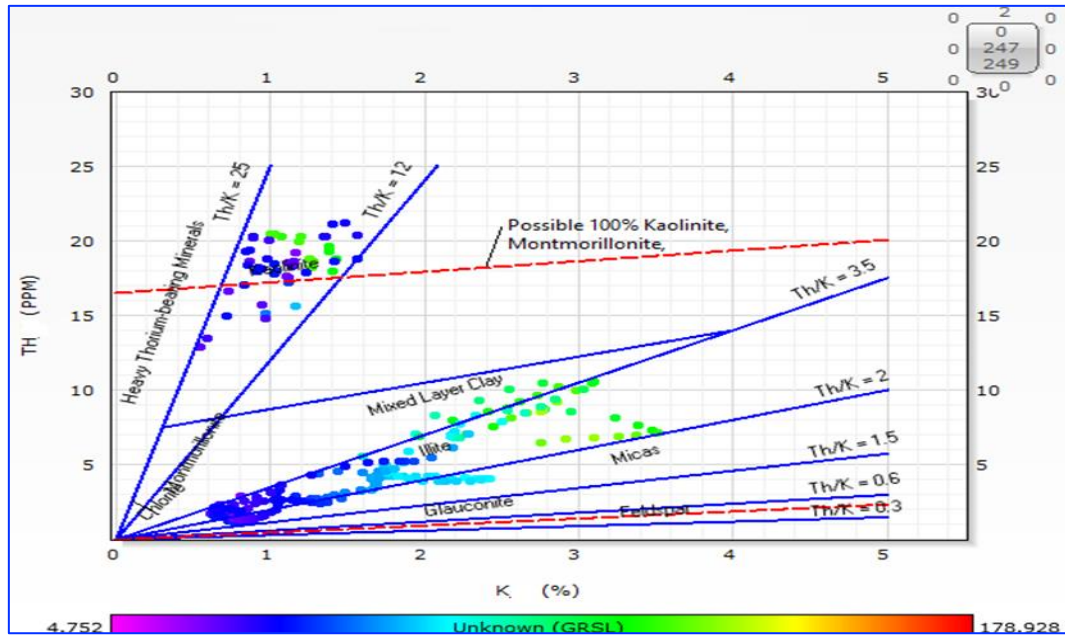
Fig. 5. Cross plot of thorium - potassium, used to identify clay minerals of selected samples from the unit (B)

Table 2. Clay mineral types in the study area are based on the the/K ratio.

Well	Units	Clay mineral	K %	The ppm	Th/K
North dome	A	Illite	2.6	7.4	2.8
		chlorite	0.2	2.4	12
	B	Illite	2.7	8.7	3.2
		Kaolinite	0.8	14.2	17.7
South dome	A	Illite	2.5	6.7	2.6
		chlorite	0.2	2.7	13.5
	B	Illite	2.4	7.9	3.2
		Kaolinite	0.9	18.5	20.5

The effect of the illite is due to its ability to disperse and transfer through solutions and block the pores, which is what causes it to affect oil reservoirs (Wilson et al., 2014). The dispersion is influenced by the size and thickness of the particles as well as by physical and chemical characteristics such as the capacity to exchange cations and the external surface area (Emerson and Chi, 1977), in addition to the nature of the replaceable cation and the concentration of the external solution, pH, and temperature (Wei et al., 2021). For example, it was discovered that Na-Illite has greater dispersibility than Ca-Illite due to its lower charge (Na) and weak hydrogen bonds (Na-Illite) (Wilson et al., 2014). The Kaolinite at the basal reflection (7.2Å) (Fig. 3), the cross-plot between thorium and potassium of Kaolinite in the southern dome has an average TH/K ratio of 20.5, and the northern dome has an average TH/K ratio of 17.7 (Fig. 5) and (Table 2) The effect of kaolin is the migration of fines due to the forces created when water moves through the pores of a formation during production and injection, especially when the salinity of the formation of water is low, which facilitates the separation of fine particles of kaolin and their deposition, a Reduction in porosity and permeability is achieved by reducing pore throat diameter (Russell et al., 2017).

Chlorite at the basal reflection (14.5Å) (Fig. 3), the cross-plot between thorium and potassium of chlorite in the southern dome has an average TH/K ratio of 13.5, while the northern dome has an average TH/K ratio of 12 (Fig. 4) and (Table 2). The effect of chlorite is either positive, where it can help to keep open pore networks in petroleum sandstone reservoirs by shielding the grains from pore fluids and preventing quartz cementation (Anjos et al., 1999), or negative, where chlorite can reduce porosity and permeability by reducing pore throat diameter (Nadeau, 2000).

3.2. Geochemistry

The concentrations of the major oxides in the Asmari reservoirs are (SiO_2, Al_2O_3, Fe_2O_3, CaO, MgO, Na_2O, K_2O, TiO_2, SO_3, and Cl_2), and their average (Table 3), (Fig. 6).

Table 4. the main oxides and LOI   percentage and their average   in the study area.the Samples 1 and 2 represent unit A, while the samples 3, 4, and 5 represent unit B, and the samples from the northern dome have the number 64, and samples from the southern dome have the number 65.

samples %	64-1	64-2	64-3	64-4	64-5	65-1	65-2	65-3	65-4	65-5	range	average
SiO_2	4.83	5.54	7.10	14.73	20.31	2.64	5.14	26.79	33.53	23.96	2.64-33.53	14.46
Al_2O_3	0.58	0.68	1.03	1.55	2.54	0.00	0.80	4.84	5.36	3.04	0.004-5.35	2.04
Fe2O3	1.30	2.42	2.70	2.70	1.58	0.47	0.85	2.56	3.17	1.79	0.47-3.17	1.95
CaO	34.07	33.61	32.90	26.15	30.65	42.44	30.58	18.92	10.83	18.21	10.83-42.44	27.84
MgO	7.58	7.13	6.81	7.30	6.71	4.22	6.34	6.18	4.31	7.39	4.22-7.57	6.40
Na2O	8.16	6.71	6.81	4.67	3.18	10.09	5.75	5.05	10.01	3.23	3.28-10.09	6.37
K2O	0.69	0.50	0.66	0.87	0.97	0.56	0.95	2.78	2.58	1.37	0.49-2.77	1.19
TiO2	0.03	0.12	0.14	0.17	0.17	0.03	0.11	0.37	0.42	0.19	0.026-0.41	0.17
SO3	35.11	26.77	27.20	10.14	6.70	47.81	14.54	13.10	7.38	6.29	6.28-47.81	19.50
Cl	0.68	0.59	0.56	1.25	0.68	0.59	1.56	1.61	2.18	1.13	0.55-2.18	1.08
LOI%	14.90	30.50	22.60	17.10	24.30	10.70	38.40	14.20	16.30	18.30	10.7-38.4	20.73
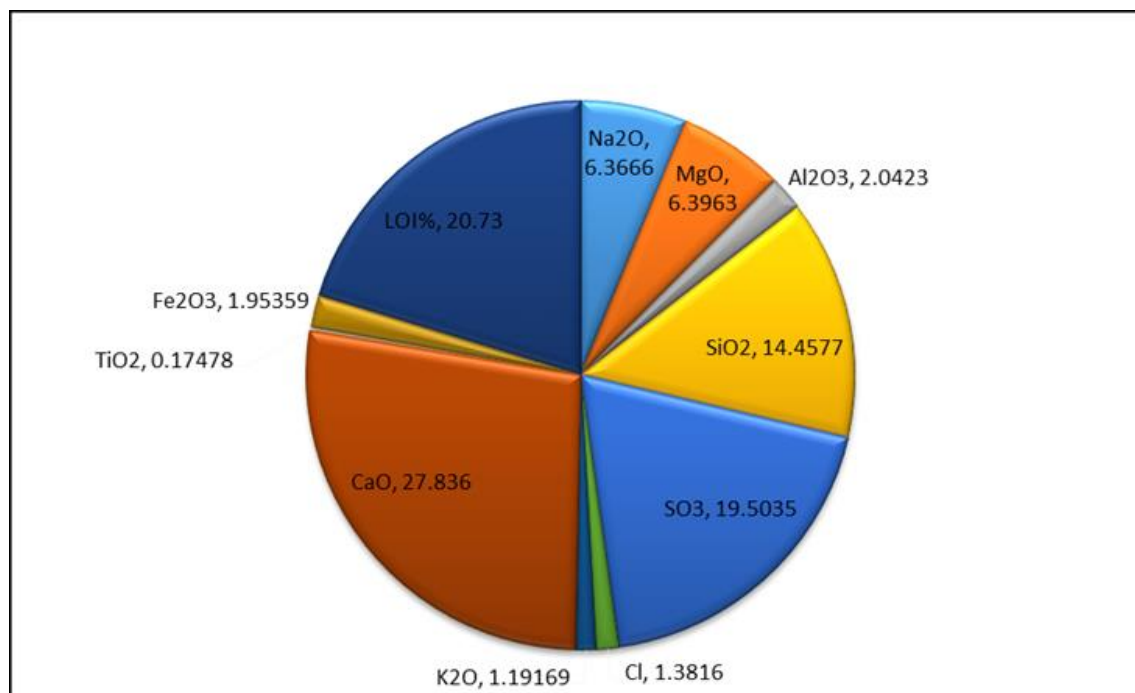
Fig. 6. The average value of the main oxides in the study area

The Silica percentage for all the studied samples ranged from (2.64% to 33.53%), with an average of (14.45%). The presence of silica is due to its entry as an essential component within the crystal structure of clay minerals in addition to its presence in the form of free silica, where it exists in the form of quartz minerals. The percentage of silica in Unit A was low When compared to unit B, it is composed of carbonate minerals, whereas unit B contains carbonate and quartz minerals.

The Alumina is found with a ratio ranging from 0.0038% to 5.35% with an average of 2.04%. The reason for the presence of alumina is that it is the primary element of the crystal structure of clay minerals, especially kaolinite, Unit A has a lower percentage of alumina than Unit B This may be because Kaolinite is absent from Unit A, while the alumina increasing in unit B as a result to presence of Kaolinite, that has been discovered by X-ray diffraction.

The Iron oxide percentage for all the studied samples ranged from 0.47% to 3.17% with an average of 1.95%. The percentage of iron increases in some samples indicating the oxidation environment (Mysen and Richet, 2019) in which these samples were deposited due to its presence within the crystalline structure of clay minerals or as adsorbed on their surfaces such as kaolinite, chlorite, and Illite (Velde, 1985) (Sandler, Taitel-Goldman and Ezersky, 2023). The percentage of iron oxide differs between the northern and southern domes in unit A, whereas there is a slight difference in the percentage of iron between the two domes in unit B, and the iron percentage in unit A is less than in unit B, as the increase in iron in the samples belonging to unit B (Fig. 6) may be due to the ionic exchange between iron and aluminum ions, especially in the kaolinite(Shaban et al., 2018), which is determined by X-ray diffraction.

The ratio of Titanium Dioxide ranged from 0.026% to 0.41% with an average of 0.17%. The presence of titanium dioxide is due to the replacement of Ti+4 ions in the crystal structure of clay minerals by Al^{3+} ions or Fe^{3+} ions as a result of the convergence of their ionic radius (Al-Saad, 2014), Or it may be found into heavy minerals (Kaminsky et al., 2008) in the study area the Unit A has a percentage of Titanium Dioxide is lower than the unit B and there is no difference in the percentage of Titanium Dioxide between the northern and southern dome in unit A, while in unit B the percentage of Titanium Dioxide in the southern dome is higher than the northern dome.

The Calcium oxide percentages ranged from 10.83% to 42.44% with an average of 27.83% Unit A has a percentage of calcite oxide higher than Unit B (Fig. 8) because most of the rocks of Unit A consist of minerals the calcium is included in their crystalline structure such as calcite, dolomite, and anhydrite while Unit B contains quartz minerals in addition to calcite, dolomite, and anhydrite, which are detected by X-ray diffraction.

The Magnesium oxide percentages ranged from 4.22% to 10.34% with an average of 6.39% Unit A has a percentage of Magnesium oxide higher than Unit B Because of the presence of a high percentage of dolomite mineral (Gregg et al., 2015) in addition to chlorite mineral (Hillier, 1993) in the samples of unit A that the Magnesium is included in their crystalline structure while Unit B contains quartz minerals in addition to calcite, dolomite, and anhydrite which are detected by X-ray diffraction.

The potassium oxide content ranges from 0.49% to 2.77% with an average 1.19%. Unit A has a lower percentage of potassium oxide than Unit B while the percentage of potassium oxide in the southern dome is higher than in the northern dome, The presence of potassium is related to the Illite mineral (Lee et al., 2017) (Al-Khalf and Al-Saad, 2019)   which is identified as one of the clay minerals in the samples being studied.

The Sodium oxide in percentages ranging from 3.18% to 10.09% with an average of 6.36% which indicates an increase in the salinity of seawater during the deposition of the Asmari group (Turki and Awadh, 2022) (Luo et al., 2019), as well as the Sodium is present in claystone as exchangeable ions in clay minerals or is adsorbed on clay mineral surfaces when the acidic function increases (He, DeSutter and Clay, 2013), for example, in the Illite mineral, the ionic exchange capacity between Ca and Na increases with the increase in salinity (Tang et al., 2022) (Endo et al., 2002).

The Sulfites are present in Asmari formation samples in percentages ranging from 6.28% to 47.81% with an average of 19.5%. This high percentage is due to the presence of an anhydrite mineral (Isah et al., 2022), which was identified by X-ray diffraction, as well as indicated to the crystallization of a Thenardite mineral is an anhydrous sodium sulfate mineral, Na_2SO_4 which occurs in arid evaporate environments (Garrett, 2001) (Steiger and Asmussen, 2008).

The Chlorine percentages ranged from 0.55% to 2.18% with an average of 3.18. (1.08%). Chlorine is one of the strongest oxidants due to its negative charge, as a result, it frequently reacts with various substances to produce chlorine salts, the most significant of which is halite (Aquilano et al., 2016) (Pedretti et al., 2022) which was identified in the study samples.

The percentage of the loss of ignition (LOI) in the study samples ranged between 10.7% to 38.4% with an average (20.75%). This ratio can be considered high when it is compared with the major element oxides. The most important causes of LOI are the evaporation of molecular water (OH +) within the crystal structure of clay minerals and the water adsorbed on their surfaces and the volatile gases as a result of The crystal structure of carbonate minerals being broken, such as carbon dioxide (CO_2) and sulfur trioxide (SO_3) As a result of the breakdown of the crystal structure of sulfate minerals and evaporates as a result of heated (Al-Saad, 2014). Fig. 7 shows the concentration of the main oxides of each element in the study area.
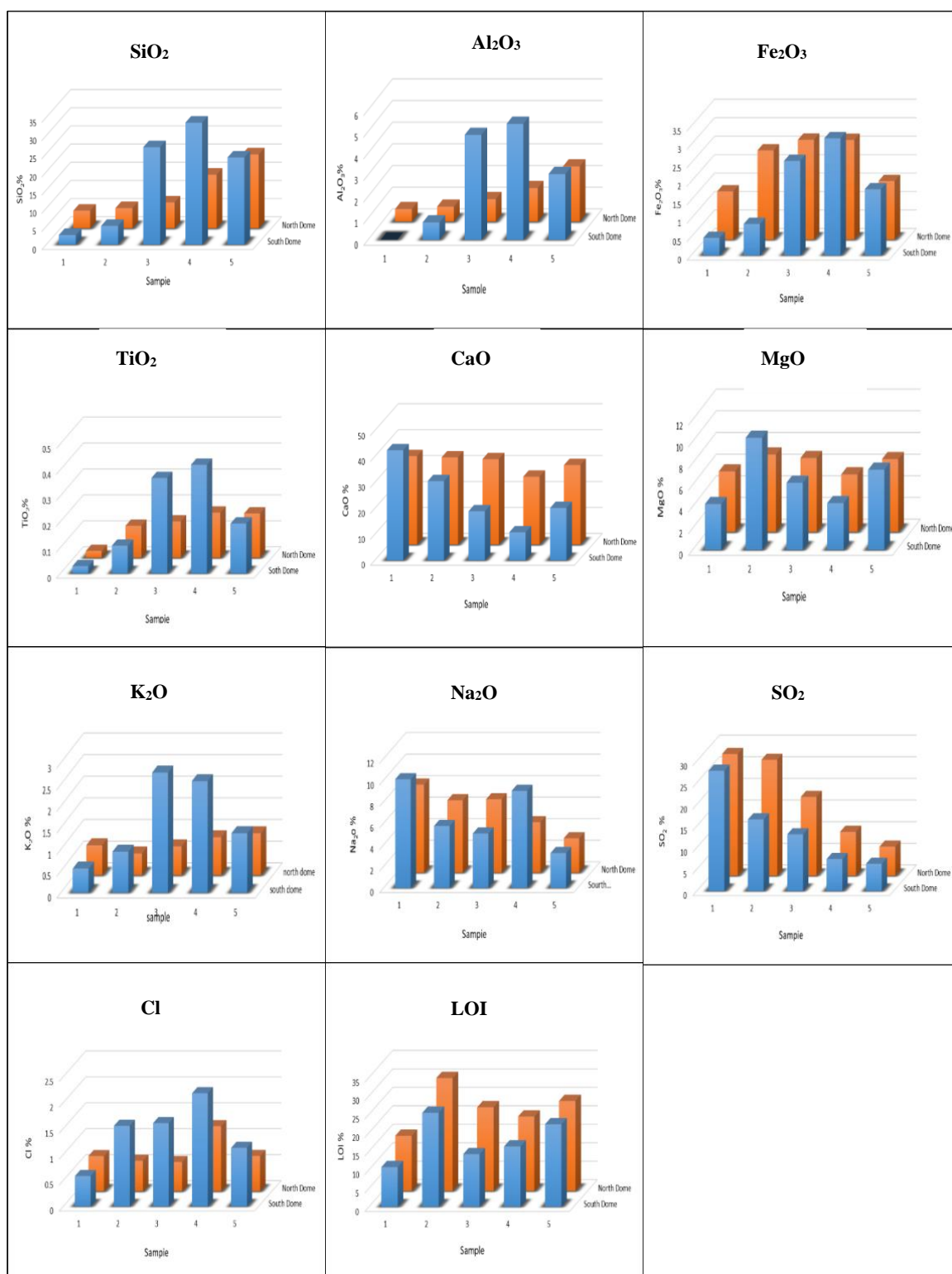
Fig. 7. Concentration of main oxides of each element in the study area. the Samples 1 and 2 represent unit A, while the samples 3, 4, and 5 represent unit B.

4. Conclusions

- X-ray diffraction mineralogy detection shows that the clay minerals are Illite, kaolinite, and chlorite, which are consistent with the results of the clay mineral thorium potassium cross diagram, and the non-clay minerals are dolomite, calcite, quartz, anhydrite, and rock salt,

- The proportion of silicon, aluminum, titanium, and potassium oxides increases in the South Dome. Whereas the North Dome has increased percentages of Ca, Mg oxides, and LOI, indicating a greater percentage of clay minerals in the South Dome.
- The positive correlation between potassium and sodium and the negative correlation between potassium and calcium indicates that the Illite is of the Na-Illite type and discovered that Na - illite has greater dispersibility than Ca-illite due to its lower charge Na and weak hydrogen bonds in Na – illite, and its existence in all samples so the Illite is the most clay mineral affecting the petrophysical properties in the study area

Acknowledgements

References

Al-Baldawi, B. A., 2015. Building A 3D Geological model Using Petrel Software for Asmari Reservoir, South Eastern Iraq, Iraqi Journal of Science, 56(2C), 1750–1762.

Al-Khalf, N. A. and Al-Saad, H. A., 2019. Mineralogy and geochemistry of recent sediments in Basrah, Southern Iraq, The Iraqi Geological Journal, 40–52.

Al-Saad, H. A., 2014. Mineralogy and Geochemistry of Claystone of Injana and Mukdadiya Formations in selected areas Eastern Maysan and Wasit and their Assessment for Normal and Lightweigt Bricks Industry', Unpublished. Ph. D. Thesis, University of Basrah, 197.

Anjos, S. M. C., De Ros, L. F. and Silva, C. M. A., 1999. Chlorite authigenesis and porosity preservation in the Upper Cretaceous marine sandstones of the Santos Basin, offshore eastern Brazil, Clay mineral cements in sandstones, 289–316.

Aquilano, D., Otálora, F., Pastero, L. and García-Ruiz, J.M., 2016. Three study cases of growth morphology in minerals: Halite, calcite and gypsum. Progress in Crystal Growth and Characterization of Materials, 62(2), 227-251.

Emerson, W. W. and Chi, C. L., 1977. Exchangeable calcium, magnesium and sodium and the dispersion of illites in water. II. Dispersion of illites in water, Soil Research, 15(3), 255–262.

Endo, T., Yamamoto, S., Honna, T. and Eneji, A.E., 2002. Sodium-calcium exchange selectivity as influenced by clay minerals and composition. Soil Science, 167(2), 117-125.

Garrett, D. E., 2001. Sodium sulfate: handbook of deposits, processing, properties, and use. Academic press.

Gregg, J.M., Bish, D.L., Kaczmarek, S.E. and Machel, H.G., 2015. Mineralogy, nucleation and growth of dolomite in the laboratory and sedimentary environment: a review. Sedimentology, 62(6), 1749-1769.

He, Y., DeSutter, T. M. and Clay, D. E., 2013. Dispersion of pure clay minerals as influenced by calcium/magnesium ratios, sodium adsorption ratio, and electrical conductivity, Soil Science Society of America Journal, 77(6), 2014–2019.

Hillier, S., 1993. Origin, diagenesis, and mineralogy of chlorite minerals in Devonian lacustrine mudrocks, Orcadian Basin, Scotland, Clays and Clay Minerals, 41(2), 240–259.

Isah, A., Arif, M., Hassan, A., Mahmoud, M. and Iglauer, S., 2022. A systematic review of Anhydrite-Bearing Reservoirs: EOR Perspective, CO2-Geo-storage and future research. Fuel, 320, 123942.

Jassim, S. Z. and Goff, J. C., 2006. Geology of Iraq. DOLIN, sro, distributed by Geological Society of London.

Kaminsky, H.A., Etsell, T.H., Ivey, D.G. and Omotoso, O., 2008. Characterization of heavy minerals in the Athabasca oil sands. Minerals Engineering, 21(4), 264-271.

Lee, J., Park, S.M., Jeon, E.K. and Baek, K., 2017. Selective and irreversible adsorption mechanism of cesium on illite. Applied geochemistry, 85, 188-193.

Luo, S., Tan, X., Chen, L., Li, F., Chen, P. and Xiao, D., 2019. Dense brine refluxing: A new genetic interpretation of widespread anhydrite lumps in the Oligocene–Lower Miocene Asmari Formation of the Zagros foreland basin, NE Iraq. Marine and Petroleum Geology, 101, 373-388.

Mysen, B. and Richet, P., 2019. Silica', in Mysen, B. and Richet, P. B. T.-S. G. and M. (Second E. (eds). Elsevier, 143–183.

Nadeau, P. H., 2000. The sleipner effect: a subtle relationship between the distribution of diagenetic clay, reservoir porosity, permeability, and water saturation', Clay Minerals, 35(1), 185–200.

Pedretti, D., Vriens, B., Skierszkan, E.K., Baják, P., Mayer, K.U. and Beckie, R.D., 2022. Evaluating dual-domain models for upscaling multicomponent reactive transport in mine waste rock. Journal of Contaminant Hydrology, 244, 103931.

Russell, T., Pham, D., Neishaboor, M.T., Badalyan, A., Behr, A., Genolet, L., Kowollik, P., Zeinijahromi, A. and Bedrikovetsky, P., 2017. Effects of kaolinite in rocks on fines migration. Journal of Natural Gas Science and Engineering, 45, 243-255.

Sandler, A., Taitel-Goldman, N. and Ezersky, V., 2023. Sources and formation of iron minerals in eastern Mediterranean coastal sandy soils – A HRTEM and clay mineral study', CATENA, 220, 106644.

Shaban, M., Sayed, M.I., Shahien, M.G., Abukhadra, M.R. and Ahmed, Z.M., 2018. Adsorption behavior of inorganic-and organic-modified kaolinite for Congo red dye from water, kinetic modeling, and equilibrium studies. Journal of Sol-Gel Science and Technology, 87, 427-441.

Steiger, M. and Asmussen, S., 2008. Crystallization of sodium sulfate phases in porous materials: The phase diagram Na_2SO_4–H_2O and the generation of stress', Geochimica et Cosmochimica Acta, 72(17), 4291–4306.

Tang, L., Li, X., Feng, H., Ma, C., Chang, Q. and Zhang, J., 2022. Infiltration of salt solutions through illite particles: Effect of nanochannel size and cation type. Colloids and Surfaces A: Physicochemical and Engineering Aspects, 641, 128581.

Turki, F. H. and Awadh, S. M., 2022. Geochemical criteria for discriminating shallow and deep environments in Oligocene-Miocene Succession, Western Iraq, The Iraqi Geological Journal, 1–15.

Velde, B., 1985. Clay minerals.

Wei, X., Pan, D., Xu, Z., Xian, D., Li, X., Tan, Z., Liu, C. and Wu, W., 2021. Colloidal stability and correlated migration of illite in the aquatic environment: The roles of pH, temperature, multiple cations and humic acid. Science of The Total Environment, 768, 144174.

Wilson, M.J., Wilson, L. and Patey, I., 2014. The influence of individual clay minerals on formation damage of reservoir sandstones: a critical review with some new insights. Clay minerals, 49(2), 147-164.